Effects of Two Familial Hypertrophic Cardiomyopathy Mutations in α-Tropomyosin, Asp175Asn and Glu180Gly, on the Thermal Unfolding of Actin-Bound Tropomyosin

Elena Kremneva,* Sabrina Boussouf,† Olga Nikolaeva,‡ Robin Maytum,† Michael A. Geeves,† and Dmitrii I. Levitsky*‡

*A. N. Bach Institute of Biochemistry, Russian Academy of Sciences, Moscow 119071, Russia; ‡A. N. Belozersky Institute of Physico-Chemical Biology, Moscow State University, Moscow 119992, Russia; and †Department of Biosciences, University of Kent at Canterbury, Canterbury, Kent CT2 7NJ, United Kingdom

ABSTRACT Differential scanning calorimetry was used to investigate the thermal unfolding of native α-tropomyosin (Tm), wild-type α-Tm expressed in *Escherichia coli* and the wild-type α-Tm carrying either of two missense mutations associated with familial hypertrophic cardiomyopathy, D175N or E180G. Recombinant α-Tm was expressed with an N-terminal Ala-Ser extension to substitute for the essential N-terminal acetylation of the native Tm. Native and Ala-Ser-Tm were indistinguishable in our assays. In the absence of F-actin, the thermal unfolding of Tm was reversible and the heat sorption curve of Tm with Cys-190 reduced was decomposed into two separate calorimetric domains with maxima at ~42 and 51°C. In the presence of phalloidin-stabilized F-actin, a new cooperative transition appears at 46–47°C and completely disappears after the irreversible denaturation of F-actin. A good correlation was found to exist between the maximum of this peak and the temperature of half-maximal dissociation of the F-actin/Tm complex as determined by light scattering experiments. We conclude that Tm thermal denaturation only occurs upon its dissociation from F-actin. In the presence of F-actin, D175N α-Tm shows a melting profile and temperature dependence of dissociation from F-actin similar to those for wild-type α-Tm. The actin-induced stabilization of E180G α-Tm is significantly less than for wild-type α-Tm and D175N α-Tm, and this property could contribute to the more severe myopathy phenotype reported for this mutation.

INTRODUCTION

Tropomyosin (Tm) is an actin-binding, α-helical coiled-coil protein that binds along the length of actin filament in both muscle and nonmuscle cells (Smillie, 1979; Lees-Miller and Helfman, 1991; Perry, 2001). Muscle cells express two major isoforms of Tm (α and β), each containing 284 residues. Smooth and skeletal muscles express different isoforms resulting from alternate splicing of the two genes (Lees-Miller and Helfman, 1991). In striated muscle cells, Tm has a well-defined regulatory function. The binding of Tm to the actin filament confers cooperativity upon the interaction of actin with myosin heads, and in combination with troponin, regulates striated muscle contraction (Gordon et al., 2000). Current views of the thin filament regulation in striated muscle, based on both biochemical and structural data, suggest that Tm can occupy three different positions or states on actin (''B'', ''blocked'' or calcium-free; ''C'', ''closed'' or calcium induced; and ''M'', myosin induced or ''open''), depending on the presence or absence of troponin, myosin, and Ca^{2+} (McKillop and Geeves, 1993; Vibert et al., 1997; Holmes, 1995; Maytum et al., 1999; Lehman et al., 2000). The movements of actin-bound Tm between these positions are believed to play a crucial role in the regulation of actomyosin interaction. More recently, models of thin filament regulation and Tm functions have been proposed (Maytum et al., 1999; Lehrer et al., 1997; Smith et al., 2003, Singh and Hitchcock-DeGregori, 2003) in which actin-bound Tm can be considered as a continuous flexible filament whose dynamic properties are modulated by external influences such as the presence of troponin and actin-bound myosin.

We are therefore interested in the flexibility of the Tm coiled-coil that we believe facilitates the rapid relocation of Tm on the actin surface. Protein flexibility can be expected to correlate with thermal instability, and therefore studies of thermal unfolding may provide valuable information on the structure of Tm both free in solution and bound to actin.

Thermal unfolding of the Tm coiled-coil can be successfully studied by different methods such as circular dichroism (CD), fluorescence, and differential scanning calorimetry (DSC). In particular, thermal denaturation of Tm from skeletal and smooth muscles has been investigated in detail by DSC (Williams and Swenson, 1981; Potekhin and Privalov, 1982; Sturtevant et al., 1991; O'Brien et al., 1996; Orlov et al., 1998). DSC is also useful for structural studies of protein-protein interactions as a direct method for measuring the thermal unfolding of proteins interacting with each other (Brandts and Lin, 1990). Recently, DSC was used to study the specific interaction of Tm with actin filaments (Levitsky et al., 2000; Kremneva et al., 2003). This demonstrated that the interaction of Tm with F-actin produces pronounced changes in the thermal unfolding of Tm, but it has no effect on the thermal unfolding of phalloidin-stabilized F-actin, which

Submitted June 30, 2004, and accepted for publication September 14, 2004.

Address reprint requests to Michael A. Geeves, Dept. of Biosciences, University of Kent at Canterbury, Canterbury, Kent CT2 7NJ, UK. Tel: 44-1227-827597; Fax: 44-1227-763912; E-mail: m.a.geeves@kent.ac.uk.

0006-3495/04/12/3922/12 $2.00

doi: 10.1529/biophysj.104.048793

denatures at a much higher temperature than Tm. It has also been found, by measuring the temperature dependence of light scattering, that thermal unfolding of smooth muscle Tm is accompanied by its dissociation from F-actin (Levitsky et al., 2000). Thus, the use of DSC in combination with other methods offers a new and promising approach for structural characterization of actin-bound Tm.

The α-Tm chain contains one cysteine residue at position 190 that can cross-link the two chains under oxidizing conditions. A high concentration of strong reductant (20 mM dithiothreitol or β-mercaptoethanol) and even denaturing conditions are normally used for reduction and labeling of the cysteine, suggesting that the cysteine thiol groups are relatively inaccessible (Lehrer, 1975; Ishii and Lehrer, 1990).

Missense mutations in α-Tm can cause familial hypertrophic cardiomyopathy (FHC; Thierfelder et al., 1994; Michele and Metzger, 2000; Seidman and Seidman, 2001). Two of the FHC α-Tm mutations (Asp175Asn and Glu180Gly) occur in residues that have been highly conserved during evolution (Thierfelder et al., 1994). Both of these FHC mutations introduce changes in surface charge in the region of the Tm molecule that has been implicated in troponin T binding and have been shown to cause partial unwinding of the Tm coiled-coil in this region (Golitsina et al., 1997). Studies on transgenic mouse lines that encode these FHC mutations in α-Tm showed that one Tm mutation (D175N) causes only a mild hypertrophy (Muthuchamy et al., 1999), whereas the other FHC mutation (E180G) leads to severe cardiac hypertrophy and death in mice (Prabhakar et al., 2001). Both Tm mutations had a small effect on the thermal stability of Tm (measured using CD) but caused increased local flexibility or decreased local stability in the regions surrounding the mutations (Golitsina et al., 1997). The mechanism by which these mutations cause cardiac hypertrophy remains an important question. Furthermore, it is not currently understood why the E180G mutation is much more disruptive than the D175N mutation, even though both mutations are in close proximity to each other.

In this work we have used DSC to characterize the thermal unfolding of skeletal α-Tm and its FHC mutants, D175N α-Tm and E180G α-Tm, both free in solution and bound to F-actin. We have shown that actin stabilizes the C-terminal part of all three Tms and that thermal denaturation of Tm only occurs upon its dissociation from F-actin. The actin-induced stabilization of E180G α-Tm is significantly less than for wild-type α-Tm and D175N α-Tm, and this could explain why this mutation causes severe FHC. The implications of these results upon the mechanism of the thermal unfolding of actin-bound Tm are discussed.

MATERIALS AND METHODS

Protein preparations

Rabbit actin was prepared by the method of Spudich and Watt (1971). Its molar concentration was determined by its absorbance at 290 nm using an $E^{1\%}$ of 6.3 cm^{-1} and a molecular mass of 42,000 Da. F-actin polymerized by the addition of 4 mM $MgCl_2$ was further stabilized by the addition of a 1.5-fold molar excess of phalloidin (Sigma Chemical, St. Louis, MO).

Native α-Tm from rabbit skeletal muscle was purified and the native α-Tm/β-Tm mixture separated by a modification of the method of Smillie (1982), using anion-exchange with a HiTrap-Q column (Pharmacia, Uppsala, Sweden) at pH 7.5 in the presence of 6 M urea.

Expression of recombinant tropomyosins

Rat-striated α-Tm was amplified from a pGEM-4 clone containing the entire gene including ≈100bp of 5′ untranslated region (gift from Dr. C. Smith, University of Oxford) using polymerase chain reaction primers designed to clone just the coding sequence and introduce this fragment via *Nde*I and *Bam*HI restriction sites into the pJC20 expression vector as described before (Maytum et al., 2000). Two different primers were designed for the N-terminal coding sequence, with one coding for three additional amino acids, Met-Ala-Ser, to produce a protein with the Ala-Ser extension, designated Sk(n2) Tm. This extension is commonly used to mimic the lack of N-terminal acetylation in *Escherichia coli*-expressed proteins (Monteiro et al., 1994). The primer designed for the 3′ C-terminal sequence was also modified to include a K279N mutation, changing the one difference in the rat sequence to match the rabbit/human sequences. Primer sequences (restriction sites shown in italics) were:

5′ *Nde*I—GGAATTC*CATATG*GACGCCATCAAGAAGAAGATGC,
5′ *Nde*I AlaSer—GGAATTC*CATATG*GCGAGCATGGACGCCATCAAGAAGAAGATGC,
5′ *Bam*HI—CGC*GGATCC*TTATATGGAAGTCATATCGTTGAGAGC.

Polymerase chain reaction-based site-directed mutagenesis was then used with these primers in combination with the following internal primers to produce the cardiomyopathy mutations D175N and E180G, as well as the cysteine knock-out C190S. Primer sequences are shown with the mutated sequences in lower case:

Sk D175N Forward 5′—CATCATCGAGAGCaatCTGGAGCGTGCGG,
Sk D175N Reverse 5′—CCGCACGCTCCAGattGCTCTCGATGATG;
Sk E180G Forward 5′—GGAGCGTGCGgggGAGAGGGCTGAG,
Sk E180G reverse 5′—CAGCCCTCTCcccCGCACGCTCCAAG;
Sk C190S Forward—GGAAGGCAAAtctGCGGAGCTTG,
Sk C190S Reverse—5′ CAAGCTCCGCagaTTTGCCTTCC.

For expression, all the clones were transformed into BL-21 DE3(pLys) and expressed and purified as previously described (Maytum et al., 2000). In brief, 1 L cultures were grown to late exponential phase and induced for 3 h with 0.4 mM IPTG. Cells were harvested and resuspended in 60 ml lysis buffer (20 mM Tris pH 7.5, 100 mM NaCl, 2mM EDTA, 1mg/L DNase, 1mg/L RNase) and lysed by passage through a French press (15,000 psi). The majority of *E. coli* proteins were precipitated by heating to 80°C for 10 min, and the precipitated protein and cell debris removed by centrifugation. The soluble Tm was then isoelectrically precipitated at pH 4.5 by addition of 0.3 M HCl. The precipitate was pelleted and resuspended in a 10–20 ml (dependent upon yield) running buffer (10 mM phosphate pH 7.0, 100 mM NaCl). This was then further purified using 2 × 5 ml Pharmacia HiTrap-Q columns in tandem, eluted with a 150–400 mM NaCl gradient, the Tm eluting at ~200–250 mM salt. Fractions were analyzed by SDS-PAGE (Laemmli, 1970), pooled, and concentrated by isoelectric precipitation. Extinction coefficients for recombinant proteins were calculated from the sequences using ANTHEPROT (Gilbert Deleage, Institut de Biologie et Chimie des Protéines-Centre National de la Recherche Scientifique). Skeletal protein concentrations were determined using an extinction coefficient E_{280nm} of 9,170 M^{-1} cm^{-1} and molecular weights of 32681.7 and 32839.8 for Sk Tm and Sk(n2) Tm; 32,680.7 and 32838.8 for Sk D175N and Sk(n2) D175N; 32609.6 and 32767.7 for Sk E180G and Sk(n2) E180G; and 32823.7 for Sk(n2) C190S.

Reduced and cross-linked tropomyosin

The content of cross-linked and reduced Tm dimers was estimated by SDS-PAGE (Laemmli, 1970) run under nonreducing conditions, in the absence of β-mercaptoethanol (BME) (Fig. 1). The gel shows samples of wild-type (wt) α-Tm and the mutant proteins after purification from *E. coli*. In each case, the proteins were almost completely cross-linked and appear as dimers (α-α). To obtain these proteins in the reduced state, they were incubated with 20 mM BME at 60°C for 60 min and then heated to 70°C for 10 min. Such treatment results in only Tm monomers on the gel (α, Fig. 1). To maintain the reduced Tm species, 1 mM BME was added to the samples.

Cosedimentation and quantitative electrophoresis

Cosedimentation assays were performed at 20°C by mixing 10 μM polymerized F-actin with 0–3 μM Tm in the standard assay buffer (20 mM Hepes, 100 mM KCl, 2 mM $MgCl_2$, 1 mM BME, pH 7.3) to a total volume of 100 μl. The actin, along with any bound protein, was then pelleted by centrifugation at 100,000 $\times$ *g* for 20 min (Beckman TL100A, Beckman Coulter, Fullerton, CA). Equivalent samples of pellet and supernatant were then separated by SDS-PAGE performed according to Laemmli (1970) using 13.5% acrylamide gels and stained with Coomassie blue G-250. Quantification of proteins was carried out by using an Epson 1640SU scanner with transparency adaptor attached to a PC. The scanner was calibrated using a Kodak neutral density step tablet and scanned images were analyzed using the Image-PC program (Scion Corp., Frederick, MD, based upon NIH Image).

Differential scanning calorimetry

DSC experiments were performed on a DASM-4M differential scanning microcalorimeter (Institute for Biological Instrumentation, Pushchino, Russia) as described earlier (Orlov et al., 1998; Levitsky et al., 2000; Kremneva et al., 2003). All measurements were carried out in 20 mM Hepes, pH 7.3, containing 100 mM KCl and 2 mM $MgCl_2$, at a scanning rate of 1 K/min. In the case of reduced Tm species, the solution also contained 1 mM BME to prevent disulfide cross-linking between the chains in the Tm homodimers. The final concentration of F-actin was 46.7 μM, and Tm concentration varied from 7.5 to 30 μM. F-actin was stabilized by the addition of a 1.5-fold molar excess of phalloidin (Sigma) to obtain a better separation of the thermal transitions of actin-bound Tm and F-actin (Levitsky et al., 2000). Specific binding of this cyclic heptapeptide to F-actin was shown to increase the temperature of the thermal denaturation of F-actin by 14°C (Levitsky et al., 2000; Le Bihan and Gicquaud, 1991). The reversibility of the thermal transitions was assessed by reheating of the sample immediately after cooling from the previous scan. The calorimetric traces were corrected for the instrumental background by subtracting a scan with buffer in both cells. The temperature dependence of the excess heat capacity was further analyzed and plotted using Origin software (MicroCal, Northampton, MA). The thermal stability of the proteins was described by the temperature of the maximum of thermal transition (T_m), and calorimetric enthalpy (ΔH_{cal}) was calculated as the area under the excess heat capacity function.

The DSC data, with instrumental baseline deducted, obtained in all the experiments were analyzed by using the software package Origin 1.16 (MicroCal). Deconvolution is based on the procedure described by Freire and Biltonen (1978). The complex endotherm may be resolved into several Gaussian distributions, each representing individual transitions, using a least-squares curve fitting procedure. Thus, the software allows for determination of the number of two-state transitions (calorimetric domains) contributing to the complex endotherm. It was found that no more than three or four independent domains are needed to obtain adequate fits. The following parameters were considered for each domain: the ΔH_{cal}, which gives the size of the transition, and T_m, which locates the midpoint of the thermal transition of the domain.

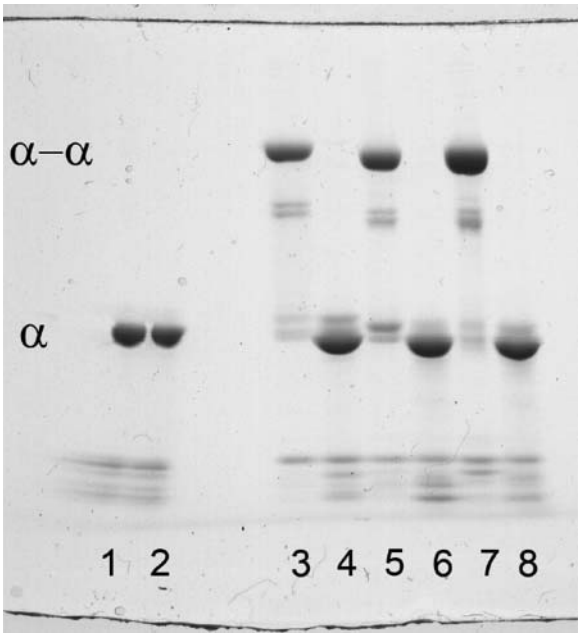

FIGURE 1 SDS-PAGE analysis under nonreducing conditions (in the absence of BME) of C190S α-Tm (*1* and *2*), wt α-Tm (*3* and *4*), D175N α-Tm (*5* and *6*), and E180G α-Tm (*7* and *8*). Lanes 1, 3, 5, and 7 represent the samples without any special treatments. Lanes 2, 4, 6, and 8 represent the Tm samples subjected to reduction procedure (incubation to 60°C for 1 h in the presence of 20 mM BME). The monomer bands are labeled as α, and the disulfide cross-linked Tm homodimers are labeled as α-α.

Light scattering

Thermally induced dissociation of Tm–F-actin complexes was detected by changes in light scattering at 90° (Wegner, 1979). All measurements were performed at 350 nm on a Cary Eclipse fluorescence spectrophotometer (Varian Australia, Mulgrave, Australia) equipped with temperature controller and thermoprobes. Light-scattering measurements were performed under the same conditions and at the same heating rate as the DSC experiments. To achieve better correspondence of the temperatures measured in the fluorimeter cells to those measured in the calorimeter cells, both instruments were calibrated by measuring the same suspension of dipalmitoylphosphatidylcholine, which showed a very sharp phase transition with a maximum at 41.2°C. Scattering of F-actin solutions containing the same concentration of actin as in the Tm–F-actin samples was measured before the experiments. This value increased proportionally with the amount of Tm bound to F-actin. When Tm dissociated from F-actin during heating, the value of the light-scattering intensity became equal to that of F-actin, because the light scattering of free Tm molecules was negligible (Wegner, 1979). Thus, a temperature-dependent decrease in light-scattering intensity of the Tm–F-actin complexes reflects dissociation of Tm from F-actin. The dissociation curves, with temperature dependence of light scattering for F-actin alone deducted, were analyzed by using the Origin software (MicroCal), according to a sigmoidal decay function (Boltzmann). The main parameter extracted from this analysis is T_{diss}, i.e., the temperature at which a 50% decrease in light scattering occurs.

RESULTS

Thermal unfolding of recombinant α-Tm

The excess heat capacity curves obtained for cross-linked or reduced recombinant wt α-Tm are presented in Fig. 2, *A* and

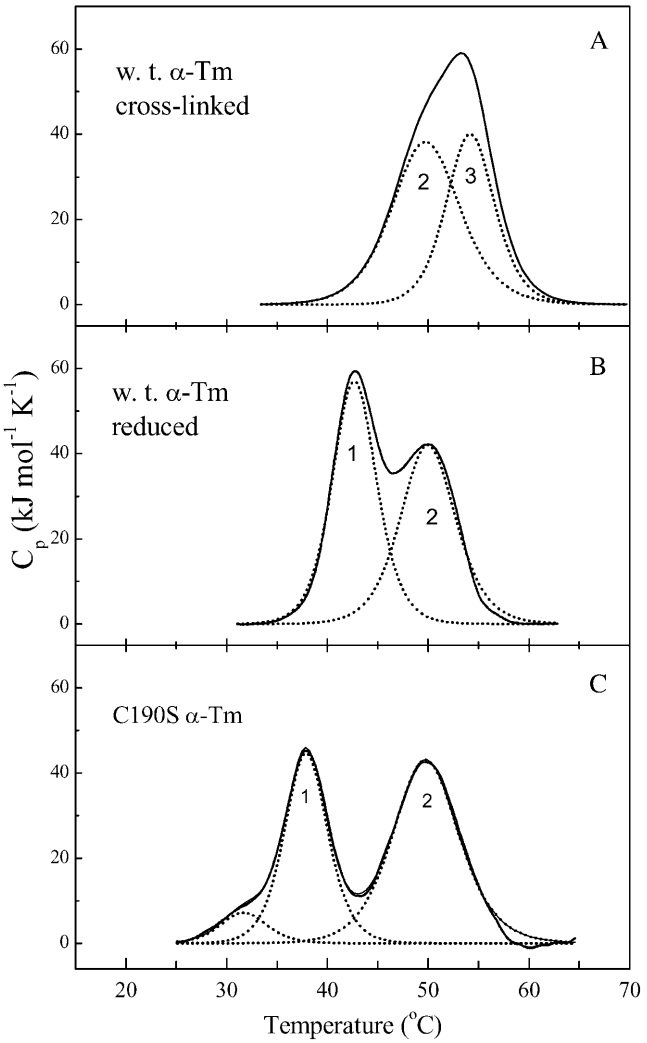

FIGURE 2 Temperature dependence of the excess heat capacity (C_p) and deconvolution analysis of the heat sorption curves of cross-linked (*A*) or reduced (*B*) recombinant α-Tm and of mutant C190S α-Tm (*C*), which is insensitive to reduction procedure (Fig. 1). The protein concentration was 20 μM. Other conditions: 20 mM Hepes, pH 7.3, 100 mM KCl, and 2 mM $MgCl_2$. The heating rate was 1 K/min. The curves were analyzed according to the non-two-state model. Solid lines represent the experimental curves after subtraction of instrumental and chemical baselines, and dotted lines represent the individual thermal transitions (calorimetric domains 1, 2, and 3) obtained from fitting the data to the non-two-state model.

B. The calorimetric traces were independent of heating rate and almost unchanged during a second heating of the samples, and therefore the thermal unfolding of Tm was fully reversible. The unfolding can therefore be considered to be at thermodynamic equilibrium and deconvolution analysis is possible. Such analysis shows that the curve of reduced wt α-Tm can be decomposed into two separate thermal transitions (calorimetric domains) with maxima at 42.7 and 50.0°C (Fig. 2 *B*). These domains represent 52% and 48%, respectively, of the total calorimetric enthalpy of wt α-Tm (Table 1). In the case of cross-linked wt α-Tm, two domains are also seen but at higher temperature with maxima at 50 and 54.3°C (Fig. 2 *A*) and correspond to 57 and 43% of the total calorimetric enthalpy (Table 1). These results are in good agreement with previously published DSC data on Tm (Williams and Swenson, 1981; Potekhin and Privalov, 1982; Sturtevant et al., 1991; Kremneva et al., 2003) and suggest that the calorimetric domain at 50–51°C corresponds to the N-terminal part of Tm and the second domain corresponds to the thermal unfolding of C-terminal part of Tm, with the thiols of Cys-190 reduced (42°C) or cross-linked between the chains of the Tm dimer (55°C).

The cross-linking occurs at the single Cys residue of Tm at position 190. To test the assumption that the shift is caused by the cross-link, we investigated the thermal unfolding of a Tm mutant with the cysteine replaced by serine (C190S α-Tm). This mutant is unable to form cross-linked Tm dimers (Fig. 1), and it demonstrates a thermal unfolding profile very similar to that seen for reduced wt α-Tm (Fig. 2 *C*). In the case of C190S α-Tm, the most thermostable calorimetric domain is absent, and the two main calorimetric domains have maxima at 37.9 and 49.8°C, respectively, with calorimetric enthalpies of 255 $\pm$ 25 and 375 $\pm$ 40 kJ/mol. A small domain with maximum at 31.7°C ($\Delta H_{cal} = 45 \pm 5$ kJ/mol) is also revealed in the C190S α-Tm (Fig. 2 *C*). This small domain could correspond to the melting of the Cys mutation-containing region of the Tm molecule.

The experiments presented here use α-Tm expressed in *E. coli* and the Tm is therefore not N-terminally acetylated as is normal for the native protein. The N-terminal acetylation is known to be essential for head-to-tail polymerization of Tm along actin. We therefore use an Ala-Ser N-terminal extension of the α-Tm, which has been shown to mimic the effect of the acetylation (Monteiro et al., 1994). We compared the thermal unfolding of recombinant wt α-Tm with that of native α-Tm obtained from rabbit skeletal muscle. There was no significant difference between the two proteins with or without the Cys cross-link.

Thermal unfolding of recombinant α-Tm carrying the FHC mutations, D175N or E180G

Fig. 3 shows the DSC curves obtained for reduced or cross-linked α-Tm FHC mutants, D175N α-Tm and E180G α-Tm. Both cross-linked Tm mutants showed melting profiles similar to that observed with oxidized wt α-Tm (cf. Fig. 2 *A*) with the exception of a small thermal transition observed at either 28°C for D175N α-Tm or at 25°C for E180G α-Tm (Fig. 3, *A* and *C*). Calorimetric enthalpy of this transition represented 8.5% and 16% of the total for D175N α-Tm and E180G α-Tm, respectively. Since these small low-temperature peaks (marked as *M* in Fig. 3, *A* and *C*) are absent in wt α-Tm, they probably correspond to the melting of a small part of Tm in the region of the mutation. Apart from this low-temperature calorimetric domain, the two cross-linked Tms are similar for wt and both mutants (see Table 1). The midpoints of the N-terminal calorimetric domains (domains

TABLE 1 Calorimetric parameters obtained from the DSC data for individual thermal transitions (calorimetric domains) of wt α-Tm, C190S α-Tm, D175N α-Tm, and E180G α-Tm*

Tm	State of Cys-190	Domain 2 (N-terminal region)		Domain 1 or 3 (C-terminal region)		Total ΔH_{cal}‡ (kJ/mol)
		T_m† (°C)	ΔH (% of total)	T_m† (°C)	ΔH (% of total)	
Wt	Cross-linked (c)	49.9	57.5	54.3	42.5	600
	Reduced (r)	50.0	48	42.7	52	640
C190S		49.8	55.5	37.9	37.5	670
D175N	c	49.2	43	53.1	48.5	520
	r	50.0	54	42.9	46	590
E180G	c	49.6	35	53.3	49	660
	r	48.8	57	39.7	43	570

*The parameters were extracted from Figs. 2 and 3.
†The error of the given values of transition temperature (T_m) did not exceed ±0.2°C.
‡The relative error of the given values of calorimetric enthalpy, ΔH_{cal}, did not exceed ±10%.

2) are essentially identical to the wt protein, whereas the C-terminal calorimetric domains (domains 3) both have their midpoints at 1°C lower (Fig. 3, *A* and *C*).

When reduced, neither α-Tm mutant demonstrates the low-temperature transition at 25–28°C (Fig. 3, *B* and *D*). This suggests that the mutations D175N and E180G disturb the Tm structure mainly when the nearby thiols of Cys-190 are cross-linked between the two chains of Tm.

In general, the thermal unfolding of reduced D175N α-Tm is essentially identical to the wt protein. The overall unfolding is similar for E180G α-Tm with two calorimetric domains (Fig. 3, *B* and *D*), but both domains have a midpoint for the transition at a lower temperature (1°C for the N-terminal, domain 2, and 3.2°C for the C-terminal, domain 1).

These results suggest that mutation E180G, unlike D175N, affects the thermal stability of the C-terminal part of Tm when Cys-190 is reduced.

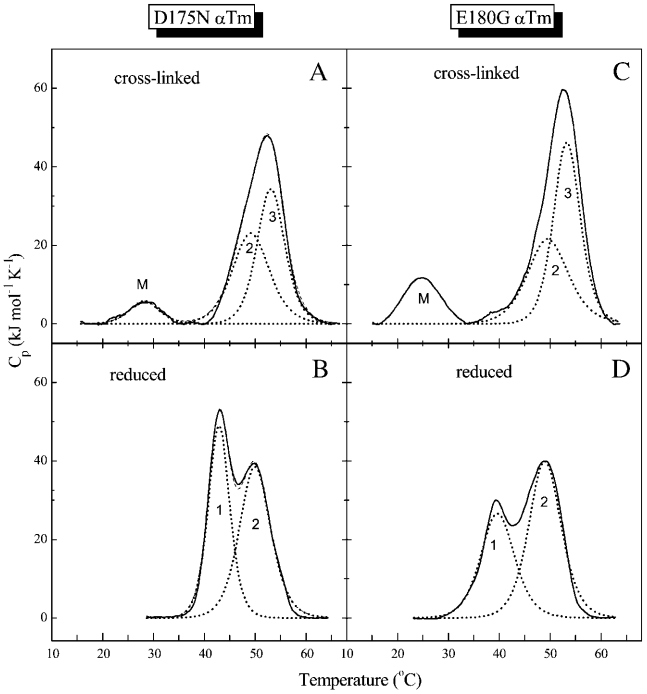

FIGURE 3 Temperature dependence of the excess heat capacity (C_p) of D175N α-Tm (*A* and *B*) and E180G α-Tm (*C* and *D*) in the cross-linked state (*A* and *C*) or in the reduced state (*B* and *D*). Solid lines represent the experimental curves after subtraction of chemical baselines, and dotted lines represent the individual thermal transitions (calorimetric domains M, 1, 2, and 3) obtained from fitting the data to the non-two-state model. Protein concentrations were 20 μM. Other conditions were the same as in Fig. 2.

The affinity of Tm for actin

The binding of oxidized wt α-Tm and its FHC mutants D175N α-Tm and E180G α-Tm to actin was investigated using cosedimentation assays. Fig. 4 plots the cooperative binding curves of the different Tms to F-actin. These curves were fitted with the Hill equation, and the concentration of free Tm at which half of the actin becomes saturated ($K_{50\%}$) was determined. The $K_{50\%}$ values obtained were 0.18 μM for wt α-Tm, 0.51 μM for D175N α-Tm, and 0.68 μM for E180G α-Tm. This shows that both FHC mutations cause a decrease in the affinity of Tm for actin with bigger effect in the case of the E180G mutation. The affinity was also measured at 200 mM KCl, and all three affinities decreased by a factor of 2, i.e., the relative affinities remained the same. The assays were repeated for reduced Tm, and no detectable change in the affinity for actin was apparent for any of the three Tms.

Thermal unfolding of α-Tm complexed with F-actin

DSC experiments with Tm–F-actin complexes were performed with reduced Tm species and in the presence of 1 mM BME to prevent cross-linking during the experiment. Where possible the experiments were done under conditions where the majority of the Tm would be bound to actin. However, since the stoichiometry of binding is 1 Tm per 7 actins, the signals for the actin-bound Tm can be relatively small. Increasing the concentration of Tm gives a better signal/noise ratio, but the increase in signal comes from non-actin-bound Tm.

The character of the thermal denaturation of wt α-Tm was noticeably changed when bound to F-actin. This is reflected in

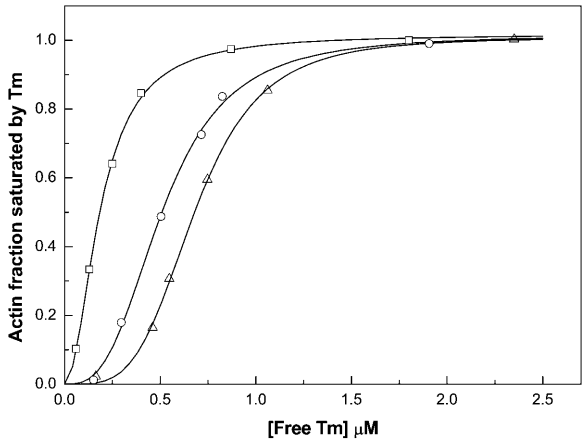

FIGURE 4 Affinity of the α-Tm constructs to actin, plotted as the fractional saturation of actin by Tm as a function of free Tm concentration. The binding of reduced recombinant wt α-Tm (□), D175N α-Tm (○), and E180G α-Tm (Δ) was carried out at 20°C in the same buffer conditions as the DSC experiments. The $K_{50\%}$ values, corresponding to the Tm concentration at which half of actin becomes saturated, are 0.18 μM, 0.51 μM, and 0.68 μM for recombinant α-Tm, D175N, and E180G α-Tm, respectively.

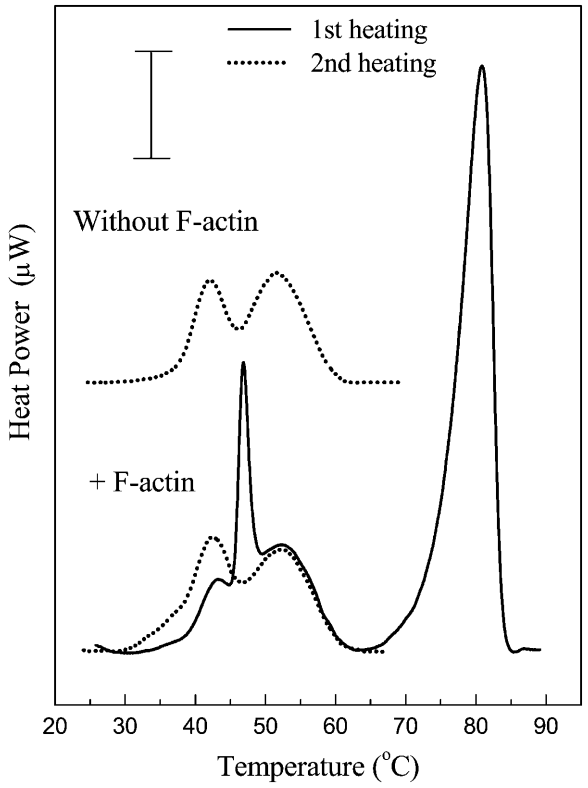

FIGURE 5 Thermal denaturation of the complex of reduced α-Tm with phalloidin stabilized F-actin. For comparison, the thermal unfolding of α-Tm in the absence of F-actin is also shown. The actin-free data shown as a dotted line were obtained by heating a corresponding sample without actin to that represented by a solid line. Conditions: 30 μM α-Tm, 46 μM F-actin, 70 μM phalloidin in 20 mM Hepes, pH 7.3, 2 mM $MgCl_2$, 100 mM KCl, and 1 mM BME. The vertical bar corresponds to 10 μW.

the appearance of a new highly cooperative thermal transition with a maximum at ~47°C (Fig. 5). The interaction of skeletal muscle α-Tm with actin had no effect on the thermal denaturation of F-actin stabilized by phalloidin, which denatures irreversibly at 80°C (Fig. 5), as previously shown for smooth muscle Tm (Levitsky et al., 2000). Thus, after heating of the Tm–F-actin complex to 90°C (i.e., after complete irreversible denaturation of actin) and subsequent cooling, only the peaks corresponding to the thermal denaturation of free reduced Tm (at 42.5 and 51°C) were observed during a second heating (*dotted line curves* on Fig. 5). Thus, we conclude that the appearance of the peak at ~47°C in the presence of F-actin reflects the thermal denaturation of actin-bound Tm.

To define the changes in the thermal unfolding of Tm induced by actin binding, we heated the Tm-actin complex three times in the calorimeter cell. First, the sample was heated to 65°C, to define the thermal unfolding of actin bound Tm but avoiding thermal denaturation of phalloidin-stabilized F-actin. Then, immediately after cooling to 5°C, the sample was heated for the second time, up to 90°C. The DSC profiles of Tm obtained from the second heating up to 65°C check the reproducibility of the Tm unfolding. Continuing to heat up to 90°C produces the irreversible denaturation of actin. A third heating was then carried out to define the thermal unfolding of Tm after irreversible denaturation of F-actin. The calorimetric curves obtained from these three heating cycles were subjected to deconvolution analysis into individual thermal transitions. In all cases, the second heating to 65°C was identical to the first heating, and therefore only the first and third heating profiles are shown.

Fig. 6 shows the results obtained with the wt Tm–F-actin complex at Tm/actin molar ratio of 1:3 (i.e., under conditions when the actin is saturated with Tm with about half of the Tm in excess). The DSC curve obtained from the first (or second) heating of the sample was decomposed into three individual thermal transitions (Fig. 6 *A*). Two of them (calorimetric domains 1 and 2) correspond to domains of actin-free reduced Tm shown in Fig. 2 *B*, whereas there is a new transition at 46.6°C. This appears only in the presence of F-actin and is absent after the irreversible denaturation of F-actin (Fig. 6 *B*). It is therefore attributed to the melting of Tm bound to F-actin, and named as transition AT (i.e., actin-Tm). Repeating the scan at different heating rates showed that the position of this AT transition did show a moderate change with heating rate (the T_m of the transition AT decreased by 1.2°C when the heating rate was decreased from 1.82 to 0.5 K/min). This indicates that the system is not fully at equilibrium. The width of the transition indicates a very cooperative process, which we attribute to a combination of the dissociation of Tm from actin concomitant with the (partial) unfolding of a stabilized fraction of the C-terminal domain.

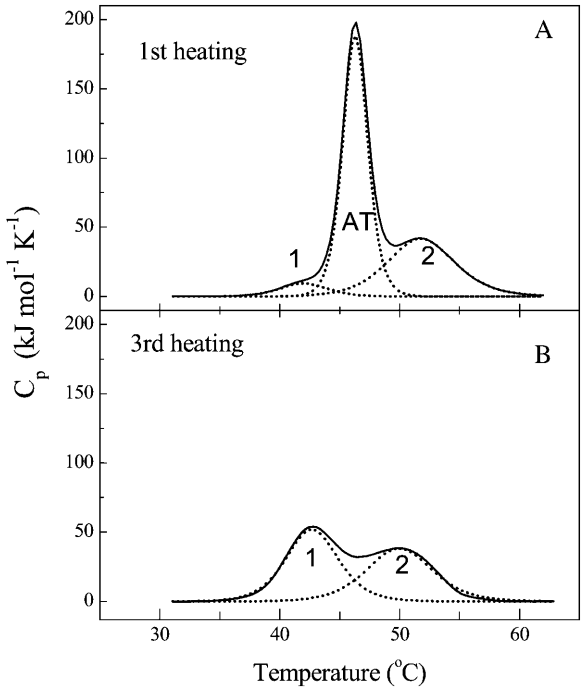

FIGURE 6 Deconvolution analysis of calorimetric curves obtained from the first (*A*) and the third (*B*) heating of the complex of reduced recombinant wt α-Tm with phalloidin-stabilized F-actin. The results of the second heating to 90°C, performed for complete irreversible denaturation of phalloidin-stabilized F-actin, were identical to those obtained from the first heating. Solid lines represent the experimental curves after subtraction of instrumental and chemical baselines, and dotted lines represent the individual thermal transitions (calorimetric domains) obtained from fitting the data to the non-two-state model. Domains 1, 2, and 3, as well as transition AT, are described in the text. Conditions: 15 μM α-Tm, 46 μM F-actin, 70 μM phalloidin, 20 mM Hepes, pH 7.3, 2 mM $MgCl_2$, 100 mM KCl, and 1 mM BME.

The calorimetric enthalpy of this new transition represents >60% of the total enthalpy of Tm. After the irreversible denaturation of F-actin during the second heating, the third heating of the sample shows the same two calorimetric domains of reduced wt α-Tm as in the absence of F-actin in Fig. 2 *B*, with no transition AT (Fig. 6 *B*). These domains represent 52% and 48%, respectively, of the total calorimetric enthalpy of Tm, and this distribution is almost identical to that obtained for α-Tm subjected to the same treatment (three heatings in the presence of BME) in the absence of actin.

We also performed this experiment at higher and lower concentrations of Tm, at a constant concentration of F-actin. In all the cases, we observed the actin-induced transition AT at 46–47°C during the first and the second heating of the sample, but the relative intensity of domain 1 significantly varied depending on the molar ratio Tm/actin. When the ratio was increased from 1:3 (at a Tm concentration of 15 μM) to 1:1.5 (at a Tm concentration of 30 μM), the relative intensity of domain 1 increased from 6% to 32%. On the other hand, at a Tm/actin molar ratio of ~1:6 (at a Tm concentration of 7.5 μM, when concentration of actin-free Tm is negligible), domain 1 was absent and only transition AT and domain 2 were present, with relative intensities of 68% and 32%, respectively (Table 2). These results are consistent with the assumption that newly observed actin-induced transition AT mainly originates from the least thermostable domain, C-terminal part of Tm with reduced Cys-190.

Thermal unfolding of actin-bound Tm mutants, D175N α-Tm and E180G α-Tm

We applied the same DSC approach described above to study the effects of FHC mutations D175N and E180G on the thermal unfolding of Tm complexed with phalloidin-stabilized F-actin. Fig. 7 shows the results obtained with D175N α-Tm bound to F-actin at a Tm/actin molar ratio of 1:6 (i.e., when almost all of Tm is bound to F-actin). In general, these results are very similar to those obtained with wt α-Tm under the same conditions. Two major domains are apparent on the first or the second heating (45.6 and 50.1°C) with relative intensities of 74 and 26% of the total (Fig. 7 *A*; Table 2). On the third heating, after irreversible denaturation of F-actin, the narrow AT peak at 45.6°C disappears and the broader domain is observed at 42.9°C (Fig. 7 *B*), very similar to that shown for free reduced D175N α-Tm in Fig. 3 *B*. Overall, D175N α-Tm is indistinguishable from wt α-Tm when bound to actin, except for a 1.5°C lower T_m for the N-terminal, domain 2.

E180G α-Tm does differ from wt α-Tm when bound to actin. A sharp transition AT appears on the thermogram at 41.4°C (Fig. 8 *A*), i.e., at a much lower temperature than in the case of wt α-Tm and D175N α-Tm under the same conditions (45.6°C), and it represents only 45% of the total enthalpy of E180G α-Tm in comparison with ~70% for wt α-Tm and D175N α-Tm (Table 2). After denaturation of actin, the sharp peak labeled AT is lost and only domains 1 and 2 are observed at 40 and 49°C, with relative intensities of 26% and 74% of the total enthalpy, respectively (Fig. 8 *B*).

Thus, these DSC results show that E180G α-Tm significantly differs from wt α-Tm and D175N α-Tm in the ability to undergo actin-induced changes in the thermal unfolding of Tm. The actin-induced transition AT occurs in E180G α-Tm at an ~4°C lower temperature and with lower enthalpy than for wt α-Tm and D175N α-Tm. This difference can be explained by lower stability of reduced domain 1 in E180G α-Tm. The interpretation, therefore, is that actin stabilizes the reduced C-terminal part of Tm with a shift in the thermogram from peak 1 to AT. The reduced domain 1 is less stable in E180G α-Tm than in wt α-Tm and D175N α-Tm, and its stabilization by actin is much less pronounced.

Thermally induced dissociation of Tm–F-actin complexes

Previous studies have shown that Tm dissociates from F-actin on heating, and this process can be studied by light scattering

TABLE 2 Calorimetric parameters of the thermal unfolding of wt α-Tm, D175N α-Tm, and E180G α-Tm in the presence of F-actin

Tm	Native F-actin	Domain 2 (N-terminal region)		Transition AT or domain 1 (C-terminal region)		Total ΔH_{cal} (kJ/mol)
		T_m (°C)	ΔH (% of total)	T_m (°C)	ΔH (% of total)	
Wt	+	51.6	32	45.6	68	880
	−	50.0	48	42.7	52	580
D175N	+	50.1	26	45.6	74	700
	−	50.1	55	42.9	45	530
E180G	+	49.2	55	41.4	45	640
	−	49.0	74	40	26	500

The parameters were obtained from deconvolution analysis of the DSC curves obtained from the first heating of the complex of reduced Tm with phalloidin-stabilized F-actin (i.e., in the presence of native F-actin) or from the third heating of the sample, after irreversible denaturation of F-actin (i.e., in the absence of native F-actin). Concentration of Tm was 7.5 μM; concentration of phalloidin-stabilized F-actin was 46 μM. The error of the T_m values did not exceed $\pm$0.2°C. The relative error of the ΔH_{cal} values did not exceed $\pm$10%. Domains 1 and 2, as well as transition AT, are described in the text.

measurements (Levitsky et al., 2000; Wegner, 1979) (Fig. 9 *A*). To confirm that the peaks labeled AT in the thermograms do represent the dissociation of Tm from actin, we examined the light-scattering signals of actin-Tm solutions. We measured the temperature dependence of dissociation of the complexes of phalloidin-stabilized F-actin with reduced wt, D175N, and E180G α-Tm at various Tm concentrations (Fig. 9, *B–D*). These measurements were performed under conditions identical to those of the DSC experiments presented in Figs. 6–8. Under these conditions, dissociation of the Tm–F-actin complexes is reversible, as the light-scattering intensity increased during cooling after the first heating and decreased again during the second heating. The light-scattering data were analyzed, and representative traces of the fits to the data are shown in Fig. 9, *B–D*. All curves were obtained from the second heating of the samples, after preheating to 60°C to ensure complete reduction of the Cys-190. It is seen that thermally induced dissociation of D175N α-Tm from F-actin is similar to that observed with wt α-Tm. Both these proteins dissociate from F-actin within the same temperature range (43–47°C, depending upon Tm concentration) close to the peak of the AT transition. The only difference between the two proteins was that the dissociation was slightly less cooperative for D175N α-Tm than for wt α-Tm (Fig. 9, *B* and *C*). On the other hand, E180G α-Tm dissociates from F-actin at a lower temperature, within the range 38–45°C (Fig. 9 *D*), depending upon the concentration of Tm used, and with lower cooperativity.

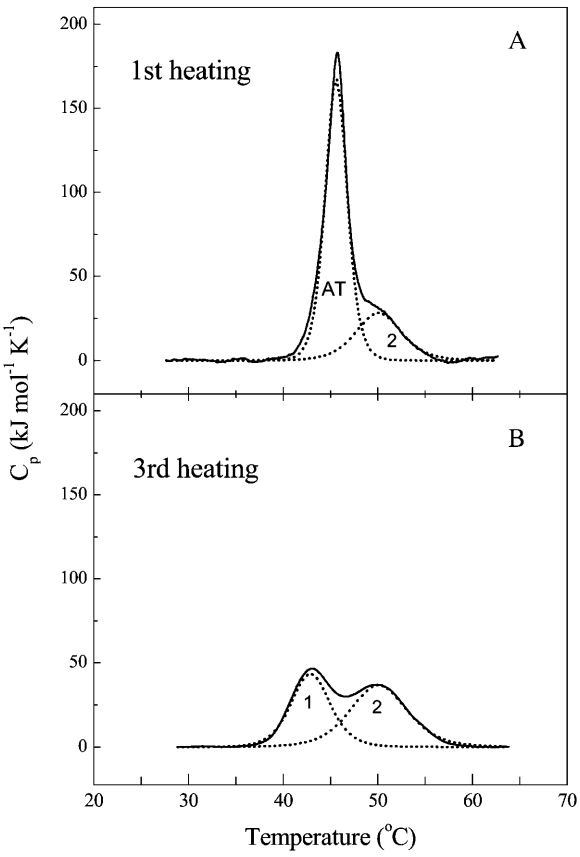

FIGURE 7 Deconvolution analysis of calorimetric curves obtained from the first heating (*A*) and the third heating (*B*) of the complex of D175N α-Tm with phalloidin-stabilized F-actin. The results of the second heating were identical to those obtained from the first heating. Concentration of D175N α-Tm was 7.5 μM. Other conditions and symbols: same as for Fig. 6.

The temperature of midpoint of dissociation of the Tm–F-actin complexes, i.e., the temperature at which a 50% decrease in light scattering occurs (T_{diss}), are presented in Table 3 and compared with the maximum temperature (T_m) of the actin-induced transition AT for the same samples studied by DSC. This comparison shows a very good correlation between the T_m and T_{diss} values (Table 3). We therefore conclude that actin-induced changes in the thermal denaturation of Tm (i.e., the appearance of the actin-induced transition AT) are associated with dissociation of Tm from F-actin.

DISCUSSION

The data presented here show that there is no difference in the actin binding and thermal unfolding properties of native and wt α-Tm expressed with the addition of Ala-Ser to the N-terminus. Ala-Ser-Tm is therefore a good mimic of native acetylated Tm. The thermal unfolding of Tm reported here agrees with previous published data from DSC (Williams and Swenson, 1981; Potekhin and Privalov, 1982; Sturtevant et al., 1991; Kremneva et al., 2003; Krishnan et al., 1978),

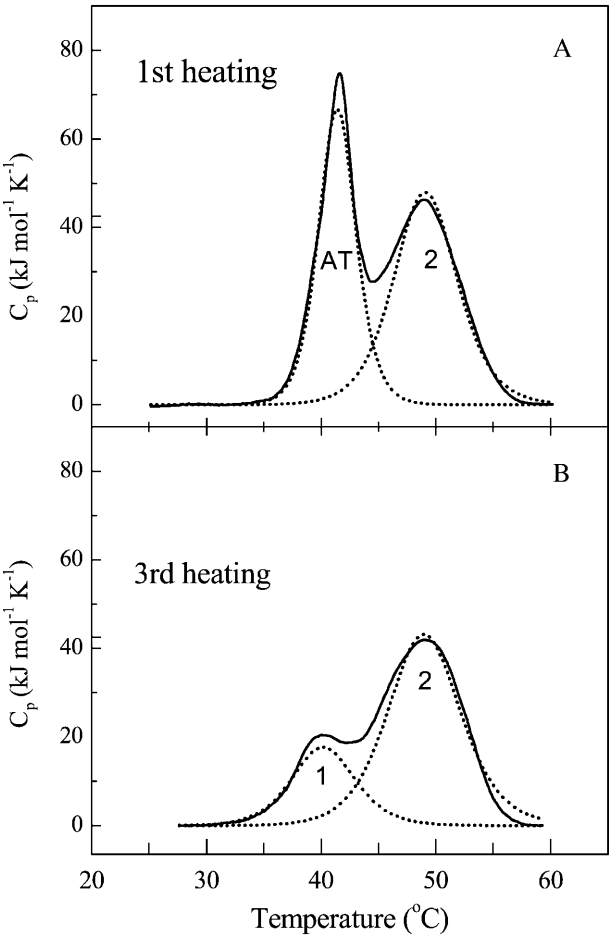

FIGURE 8 Deconvolution analysis of the DSC curves obtained from the first heating (*A*) and from the third heating (*B*) of the complex of E180G α-Tm with phalloidin-stabilized F-actin. The results of the second heating were identical to those obtained from the first heating. Concentration of E180G α-Tm was 7.5 μM. Other conditions and symbols: same as for Fig. 6.

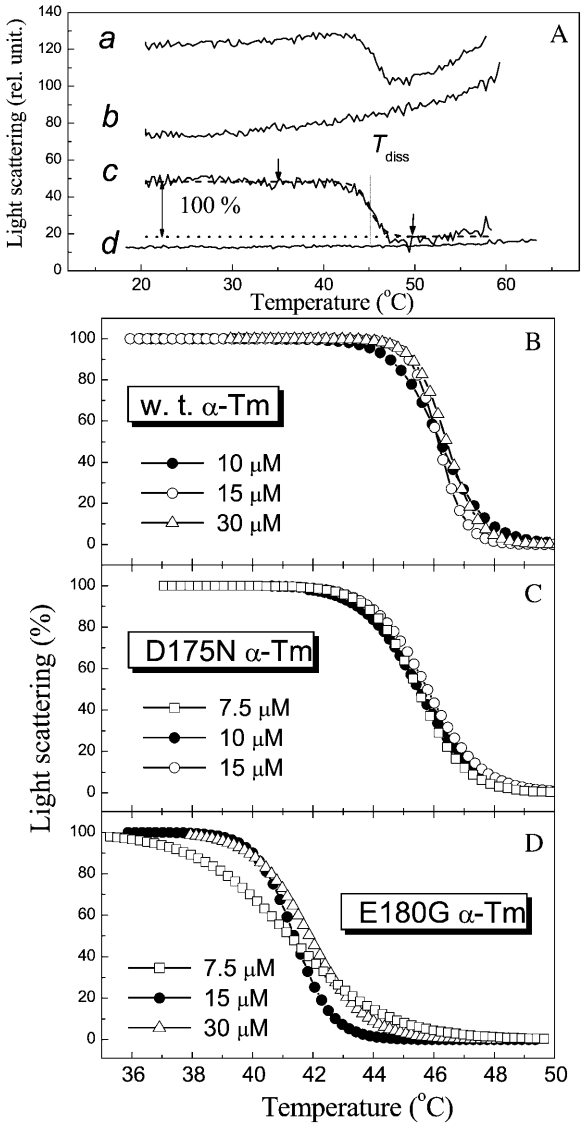

FIGURE 9 (*A*) Temperature dependence of light scattering for the complex of wt α-Tm with F-actin stabilized by phalloidin (*curve a*), for phalloidin-stabilized F-actin alone (*curve b*), and for actin-free Tm (*curve d*). Curve *c* was obtained by subtraction of curve *b* from curve *a*. A decrease in the light-scattering intensity reflects dissociation of the Tm–F-actin complex. Arrows indicate the temperature region from 35 to 50°C where dissociation occurs; 100% corresponds to the difference between light scattering of the Tm–F-actin complex and that of the mixture of F-actin with denatured Tm obtained after dissociation of the complex. T_{diss} is the temperature of half-maximal dissociation of the Tm–F-actin complex, i.e., the temperature at which a 50% decrease in light scattering occurs. (*B–D*) Normalized temperature dependence of dissociation of the F-actin complexes with reduced wt α-Tm (*B*), D175N α-Tm (*C*), and E180G α-Tm (*D*) obtained at various molar ratios Tm/actin. For ease of viewing, only the fitted curves are shown. Actin concentration 46 μM; concentration of Tm is indicated for each curve. Conditions were the same as for DSC experiments presented in Figs. 6–8. Heating rate was 1°C/min.

CD (Golitsina et al., 1997; Hitchcock-DeGregori et al., 2002) and fluorescence studies (Golitsina et al., 1997). The skeletal muscle α-Tm isoform melts in two domains with similar enthalpies of unfolding. The N-terminal domain of Tm (domain 2) melts with a midpoint of ~50°C. The C-terminal domain can be stabilized by cross-linking the cysteines at position 190. When cross-linked, this domain is the most stable and melts at ~54°C (domain 3), and when reduced is the least stable and unfolds at ~42°C (domain 1). This interpretation was confirmed by the C190S mutant.

Recent mutation and deletion experiments show that tropomyosin has many regions of varying stability, and the regions of stable coiled-coil are interrupted by less stable segments (Hitchcock-DeGregori et al., 2002; Singh and Hitchcock-DeGregori, 2003; Landis et al., 1999). Multiple independent unfolding domains in tropomyosin were identified using CD and fluorescence (Ishii et al., 1992; Ishii, 1994). Potekhin and Privalov (1982) in their DSC studies on skeletal α-Tm homodimer revealed seven cooperative blocks (calorimetric domains) with different thermal stability: three domains in the N-terminal part, three domains in the C-terminal part, and one small domain between the N- and C-terminal parts. Other authors simplified the problem and

TABLE 3 Comparison of maximum temperature (T_m) of the actin-induced thermal transition AT measured by DSC and the temperature of half-maximal dissociation (T_{diss}) of the complexes of Tm and its mutants with F-actin obtained at various Tm concentrations

Tm species	Tm concentration (μM)	T_m (°C)	T_{diss} (°C)
Recombinant wt α-Tm	5	ND	43.1 ± 0.2
	7.5	45.6	44.1 ± 0.2
	10	ND	46.2 ± 0.1
	15	46.4	46.2 ± 0.1
	30	46.9	46.4 ± 0.1
D175N α-Tm	7.5	45.6	45.5 ± 0.1
	10	45.9	45.5 ± 0.1
	15	46.5	45.8 ± 0.2
E180G α-Tm	7.5	41.4	41.2 ± 0.1
	15	41.7	41.4 ± 0.1
	30	42.0	41.9 ± 0.2
C190S α-Tm	7.5	42.4	41.7 ± 0.1
	10	43.3	42.0 ± 0.2

Values obtained from two to four independent measurements are shown. The absolute error of the given T_m values did not exceed ±0.2°C. The values of T_{diss} were calculated from light-scattering data presented in Fig. 9, *B–D*. Actin concentration was constant and equal to 46 μM.
ND, not determined.

considered only two main parts in the Tm molecule, which are clearly distinguished in their thermal stability, i.e., the N-terminal part and the C-terminal part in either of two states, reduced and cross-linked (Williams and Swenson, 1981; Sturtevant et al., 1991). In our studies, we followed this approach, especially as no more than three independent thermal transitions (calorimetric domains) were needed to obtain adequate fits during deconvolution of all the curves studied. The analysis does suggest that two unfolding domains have similar enthalpies of unfolding, but this does not mean that these represent the N- and C-terminal halves of the molecule.

As reported for smooth muscle isoform, actin stabilizes the reduced C-terminal domain of Tm by ~3°C, and this domain unfolds and Tm dissociates in a single cooperative process. This was demonstrated by the close correspondence between the midpoint of the thermally induced dissociation of Tm from actin and the new cooperative unfolding transition seen in the thermogram in the presence of actin (Table 3 and Levitsky et al., 2000). The thermal unfolding of Tm in the Tm–F-actin complex is completely reversible up to the denaturation of F-actin, as shown by repeated heatings up to 65°C. However, the binding of Tm to actin is known to be a very cooperative process, occurring as an initiation-polymerization reaction (Wegner, 1979, and Fig. 4), and thus it can be presumed that dissociation is also highly cooperative. The unfolding transition is therefore also very cooperative and not expected to occur as an equilibrium process. Once Tm begins to dissociate, Tm will dissociate from the whole filament. From our data alone it is not possible to distinguish whether a), Tm begins to unfold and this triggers cooperative dissociation followed by complete unfolding of the C-terminal region; or b), dissociation occurs cooperatively and the C-terminal region, once dissociated, is now above its thermal transition and rapidly unfolds. Note that dissociation profiles show no dependence on Tm concentration over quite a wide range (at least 10–30 μM), whereas a simple equilibrium dissociation should show a concentration dependence. This data, together with observation that thermal unfolding of actin-bound tropomyosin depends on the heating rate, thus confirms that the system is not at equilibrium during the transition, and a detailed thermodynamic analysis of the process is therefore invalid. Only the midpoint of the transition can be used as an indication of the temperature of the transition. The N-terminal domain unfolds after actin dissociates, and therefore appears unaffected by actin, as does the C-terminal domain when cross-linked (data not shown).

Analysis of the E180G and D175N mutations do show novel features. We show that both E180G and D175N bind actin with a weaker affinity than wt protein. These results contrast with those of Golitsina et al. (1997), who reported that only E180G resulted in a 2–3-fold loss of actin affinity. However, they used bacterially expressed Tm without the Ala-Ser extension on the N-terminus and thus had a very much weaker affinity for actin. Actin binding was induced by the presence of troponin in the samples, which increases Tm affinity for actin by 2–3 orders of magnitude (Cho and Hitchcock-DeGregori, 1991; Wegner and Walsh, 1981; Hill et al., 1992). Bing et al. (1997) did use similar constructs to those used here with the Ala-Ser extension. They reported a similar lower affinity of E180G Tm for F-actin compared to wt Tm, but saw no significant change in the affinity of D175N Tm. However, under the lower salt (50 mM KCl) conditions used by Bing et al. (1997), the wt Tm and D175N Tm affinities were both very tight (~0.1 μM) and at the limit of the resolution of the method. The values at 0.1 and 0.2 M KCl reported here are within the range that is well-defined by our cosedimentation assays.

In the absence of actin, both D175N and E180G mutations produce a small locally unstable region of Tm that unfolds at 28°C or at 25°C, respectively, when the Tm is oxidized. This small unstable region is not observed with reduced Tm, and is therefore induced by the nearby cross-link at Cys-190. Apart from this local instability, D175N Tm is indistinguishable from the wt Tm in the absence and presence of actin. The thermal stability, therefore, does not provide any indication as to why this mutation produces a cardiomyopathy.

In contrast. the reduced C-terminus of E180G Tm is less stable than wt Tm (by ~3°C) and only stabilized by actin by ~1°C. The AT transition occurs at 41–42°C, ~4° lower than for the wt Tm or D175N Tm.

These results mean that the reduced C-terminus of wt Tm is relatively unstable in solution, and given the width of the transition, is on the edge of its unfolding transition at resting body temperature (37°C, see Fig. 3 *D*). It is, however, 1–2°C

more stable and has a narrower transition range when bound to actin. Thus E180G appears to cause a significant loss of stability of the C-terminal part of Tm both free and bound to actin, and the midpoint of Tm dissociation/unfolding is only 3–4°C above resting body temperature. The E180G Tm may be relatively stable when bound to actin under normal resting condition, but during vigorous muscle activity, muscle temperature can increase by >2°C and similar elevated temperatures occur during fever. It is therefore possible that the loss of stability of the actin-bound E180G Tm could contribute to the long-term development of myopathy. The partial loss of E180G Tm from the thin filament would result in the inability to relax a sarcomere, which could then result in severe local overcontraction and ultrastructural damage. The occurrence of patches of myocyte disarray has been implicated in the pathology of FHC, with arrhythmias in heart contraction generated by sections of noncontracting muscle being a potential cause of sudden death (Varnava et al., 2001). In future studies it will be important to assess whether troponin, or any other thin filament protein, can provide any additional stability to the mutant Tms, either bound to actin or free in solution. Preliminary DSC studies suggest that the interaction of troponin with actin-bound Tm can provide some additional stability to Tm, but only in the absence of calcium (Kremneva et al., 2003).

The data presented demonstrate that DSC is capable of monitoring the global unfolding of two domains of Tm when bound to actin or when free in solution. As such, the approach is complementary but distinct from the use of CD and fluorescently labeled Tm. CD is of limited use in the presence of actin as the signal from the sevenfold molar excess of actin dominates the signal. Fluorescent labels can be used in the presence of actin but may report only the local unfolding of regions close to the label. As an approach for use with cardiomyopathy mutations, fluorescence labels need to be used with caution since the label may cause local changes in thermal stability of the same order as those introduced by the myopathy mutation, which by their nature can be rather subtle.

We thank Valeriya Mikhailova for her help in performing DSC experiments, Chris Smith (University of Oxford) for the gift of the α-Tm cDNA, Manfred Konrad (Max-Planck-Institut, Gottingen, Germany) for help with the production of α-Tm mutants, Nancy Adamek for the preparation of actin, and Sam Lehrer (Boston Biomedical Research Institute, Boston, MA) for comments on the manuscript.

This work was supported by the Wellcome Trust (grants 066115 to D.I.L and M.A.G., and 070021 to M.A.G.), the British Heart Foundation (studentship No. 2000014 to S.B.), the Russian Foundation for Basic Research (grants 03-04-48237 to D.I.L. and 03-04-06207 to E.K.), and by the Program for the Support of Scientific Schools in Russia (grant NSH-813.2003.4 to D.I.L).

REFERENCES

Bing, W., C. S. Redwood, I. F. Purcell, G. Esposito, H. Watkins, and S. B. Marston. 1997. Effects of two hypertrophic cardiomyopathy mutations in alpha-tropomyosin, Asp175Asn and Glu180Gly, on Ca^{2+} regulation of thin filament motility. *Biochem. Biophys. Res. Commun.* 236:760–764.

Brandts, J. F., and L.-N. Lin. 1990. Study of strong to ultratight protein interactions using differential scanning calorimetry. *Biochemistry.* 29:6927–6940.

Cho, Y. J., and S. E. Hitchcock-DeGregori. 1991. Relationship between alternatively spliced exons and functional domains in tropomyosin. *Proc. Natl. Acad. Sci. USA.* 88:10153–10157.

Freire, E., and R. L. Biltonen. 1978. Statistical mechanical deconvolution of thermal transitions in macromolecules. I. Theory and application to homogeneous systems. *Biopolymers.* 17:463–479.

Golitsina, N. L., Y. An, N. J. Greenfield, L. Thierfelder, K. Iizuka, J. G. Seidman, C. E. Seidman, S. S. Lehrer, and S. E. Hitchcock-DeGregori. 1997. Effects of two familial hypertrophic cardiomyopathy-causing mutations on α-tropomyosin structure and function. *Biochemistry.* 36:4637–4642. (See also corrections to this article in *Biochemistry.* 1999. 38:3850.)

Gordon, A. M., E. Homsher, and M. Regnier. 2000. Regulation of contraction in striated muscle. *Physiol. Rev.* 80:853–924.

Hill, L. E., J. P. Mehegan, C. A. Butters, and L. S. Tobacman. 1992. Analysis of troponin-tropomyosin binding to actin. Troponin does not promote interactions between tropomyosin molecules. *J. Biol. Chem.* 267:16106–16113.

Hitchcock-DeGregori, S. E., Y. Song, and N. J. Greenfield. 2002. Functions of tropomyosin's periodic repeats. *Biochemistry.* 41:15036–15044.

Holmes, K. C. 1995. The actomyosin interaction and its control by tropomyosin. *Biophys. J.* 68:2–7.

Ishii, Y. 1994. The local and global unfolding of coiled-coil tropomyosin. *Eur. J. Biochem.* 221:705–712.

Ishii, Y., S. Hitchcock-DeGregori, K. Mabuchi, and S. S. Lehrer. 1992. Unfolding domains of recombinant fusion alpha alpha-tropomyosin. *Protein Sci.* 1:1319–1325.

Ishii, Y., and S. S. Lehrer. 1990. Excimer fluorescence of pyrenyliodoacetamide-labeled tropomyosin: a probe of the state of tropomyosin in reconstituted muscle thin filaments. *Biochemistry.* 29:1160–1166.

Kremneva, E. V., O. P. Nikolaeva, N. B. Gusev, and D. I. Levitsky. 2003. Effects of troponin on the thermal unfolding of actin-bound tropomyosin. *Biochemistry (Mosc.).* 68:802–809.

Krishnan, K. S., J. F. Brandts, and S. S. Lehrer. 1978. Effects of an interchain disulfide bond on tropomyosin structure: differential scanning calorimetry. *FEBS Lett.* 91:206–208.

Landis, C., N. Back, E. Homsher, and L. S. Tobacman. 1999. Effects of tropomyosin internal deletions on this filament function. *J. Biol. Chem.* 274:31279–31285.

Laemmli, U. K. 1970. Cleavage of structural proteins during the assembly of the head of bacteriophage T4. *Nature.* 227:680–685.

Le Bihan, T., and C. Gicquaud. 1991. Stabilization of actin by phalloidin: a differential scanning calorimetric study. *Biochem. Biophys. Res. Commun.* 181:542–547.

Lees-Miller, J. P., and D. M. Helfman. 1991. The molecular basis for tropomyosin isoform diversity. *Bioessays.* 13:429–437.

Lehman, W., V. Hatch, V. Korman, M. Rosol, L. Thomas, R. Maytum, M. A. Geeves, J. E. Van Eyk, L. S. Tobacman, and R. Craig. 2000. Tropomyosin and actin isoforms modulate the localization of tropomyosin strands on actin filaments. *J. Mol. Biol.* 302:593–606.

Lehrer, S. S. 1975. Intramolecular crosslinking of tropomyosin via disulfide bond formation: evidence for chain register. *Proc. Natl. Acad. Sci. USA.* 72:3377–3381.

Lehrer, S. S., N. L. Golitsina, and M. A. Geeves. 1997. Actin-tropomyosin activation of myosin subfragment 1 ATPase and thin filament cooperativity. The role of tropomyosin flexibility and end-to-end interactions. *Biochemistry.* 36:13449–13454.

Levitsky, D. I., E. V. Rostkova, V. N. Orlov, O. P. Nikolaeva, L. N. Moiseeva, M. V. Teplova, and N. B. Gusev. 2000. Complexes of smooth muscle tropomyosin with F-actin studied by differential scanning calorimetry. *Eur. J. Biochem.* 267:1869–1877.

Maytum, R., M. A. Geeves, and M. Konrad. 2000. Actomyosin regulatory properties of yeast tropomyosin are dependent upon N-terminal modification. *Biochemistry.* 39:11913–11920.

Maytum, R. M., S. S. Lehrer, and M. A. Geeves. 1999. Cooperativity and switching within the three-state model of muscle regulation. *Biochemistry.* 38:1102–1110.

McKillop, D. F., and M. A. Geeves. 1993. Regulation of the interaction between actin and myosin subfragment-1: evidence for three states of the thin filament. *Biophys. J.* 65:693–701.

Michele, D. E., and J. M. Metzger. 2000. Physiological consequences of tropomyosin mutations associated with cardiac and skeletal myopathies. *J. Mol. Med.* 78:543–553.

Monteiro, P. B., R. C. Lataro, J. A. Ferro, and F. C. Reinach. 1994. Functional α-tropomyosin produced in *Escherichia coli*: a dipeptide extension can substitute the amino-terminal acetyl group. *J. Biol. Chem.* 269:10461–10466.

Muthuchamy, M., K. Pieples, P. Rethinasamy, B. Hoit, I. Grupp, G. Boivin, B. Wolska, C. Evans, R. J. Solaro, and D. F. Wieczorek. 1999. Mouse model of a familial hypertrophic cardiomyopathy mutation in alpha-tropomyosin manifests cardiac dysfunction. *Circ. Res.* 85:47–56.

O'Brien, R., J. M. Sturtevant, J. Wrabl, M. E. Holtzer, and A. Holtzer. 1996. A scanning calorimetric study of unfolding equilibria in homodimeric chicken gizzard tropomyosins. *Biophys. J.* 70:2403–2407.

Orlov, V. N., E. V. Rostkova, O. P. Nikolaeva, V. A. Drachev, N. B. Gusev, and D. I. Levitsky. 1998. Thermally induced chain exchange of smooth muscle tropomyosin dimers studied by differential scanning calorimetry. *FEBS Lett.* 433:241–244.

Perry, S. V. 2001. Vertebrate tropomyosin: distribution, properties and function. *J. Muscle Res. Cell Motil.* 22:5–49.

Potekhin, S. A., and P. L. Privalov. 1982. Co-operative blocks in tropomyosin. *J. Mol. Biol.* 159:519–535.

Prabhakar, R., G. P. Boivin, I. L. Grupp, B. Hoit, G. Arteaga, R. J. Solaro, and D. F. Wieczorek. 2001. A familial hypertrophic cardiomyopathy α-tropomyosin mutation causes severe cardiac hypertrophy and death in mice. *J. Mol. Cell. Cardiol.* 33:1815–1828.

Seidman, J. G., and C. Seidman. 2001. The genetic basis for cardiomyopathy: from mutation identification to mechanistic paradigms. *Cell.* 104:557–567.

Singh, A., and S. E. Hitchcock-DeGregori. 2003. Local destabilization of the tropomyosin coiled coil gives the molecular flexibility required for actin binding. *Biochemistry.* 42:14114–14121.

Smillie, L. B. 1979. Structure and functions of tropomyosins from muscle and non-muscle sources. *Trends Biochem. Sci.* 4:151–155.

Smillie, L. B. 1982. Preparation and identification of α and β tropomyosin. *Methods Enzymol.* 85:234–241.

Smith, D. A., R. Maytum, and M. A. Geeves. 2003. Cooperative regulation of myosin-actin interactions by a continuous flexible chain. I. Actin-tropomyosin systems. *Biophys. J.* 84:3155–3167.

Spudich, J. A., and S. Watt. 1971. The regulation of rabbit skeletal muscle contraction. I. Biochemical studies of the interaction of the tropomyosin-troponin complex with actin and the proteolytic fragments of myosin. *J. Biol. Chem.* 246:4866–4871.

Sturtevant, J. M., M. E. Holtzer, and A. Holtzer. 1991. A scanning calorimetric study of the thermally induced unfolding of various forms of tropomyosin. *Biopolymers.* 31:489–495.

Thierfelder, L., H. Watkins, C. MacRae, R. Lamas, W. McKenna, H. P. Vosberg, J. G. Seidman, and C. E. Seidman. 1994. Alpha-tropomyosin and cardiac troponin T mutations cause familial hypertrophic cardiomyopathy: a disease of the sarcomere. *Cell.* 77:701–712.

Varnava, A. M., P. M. Elliott, C. Baboonian, F. Davison, M. J. Davies, and W. J. McKenna. 2001. Hypertrophic cardiomyopathy: histopathological features of sudden death in cardiac troponin T disease. *Circulation.* 104:1380–1384.

Vibert, P., R. Craig, and W. Lehman. 1997. Steric-model for activation of muscle thin filaments. *J. Mol. Biol.* 266:8–14.

Wegner, A. 1979. Equilibrium of the actin-tropomyosin interaction. *J. Mol. Biol.* 131:839–853.

Wegner, A., and T. P. Walsh. 1981. Interaction of tropomyosin-troponin with actin filaments. *Biochemistry.* 20:5633–5642.

Williams, D. L., and C. A. Swenson. 1981. Tropomyosin stability: assignment of thermally induced conformational transitions to separate regions of the molecule. *Biochemistry.* 20:3856–3864.